

INFLUENCE OF COLLISIONS OF SMALL PARTICLES WITH LARGE PARTICLES ON THE
PROPAGATION OF SHOCK WAVES IN TWO-PHASE, TWO-FRACTION AEROSOLS

T. R. Amanbaev and A. I. Ivandaev

UDC 532.529

We propose to investigate a flow of an aerocolloidal mixture of a gas with two particulate fractions (small and large particles) within the scope of the assumptions of the mechanics of multiphase media [1], where the mixture of the gas and small particles can be regarded as a single-velocity, single-temperature continuum with its own specific thermo-physical properties (constituting the effective gas). We consider different methods of taking into account the influence of the small particles on the interaction between the effective gas and the large particles, and we make a comparative analysis of these methods. We discuss certain results of calculations of shock structures in aerosols containing small and large particles. Previous papers report investigations of the structure of shock waves in a monodisperse aerocolloid containing inert particles [2] and in a gas-droplet mixture (including a polydisperse mixture) in the presence of phase transitions [3, 4]. Other studies have dealt with the influence of droplet breakup on flow in the relaxation zone of a shock wave [5] and the influence of the cooling of small particles on large droplets [6]. A detailed survey of papers on shock propagation in aerosols may be found in [7].

The formulation of the equation of motion of the investigated aerosol does not present any special difficulty within the framework of the stated assumptions. Here we give only the equations of state and the laws governing the interaction of the phases.

1. EQUATIONS OF STATE

We assume that the gas is calorically ideal and that the solid (particulate) phases are incompressible media with constant specific heats. We then write the equations of state of the effective gas and the large particles in the form

$$p = \rho_1^0 R_1 T_1, \quad e_1 = c_1 T_1, \quad e_2 = c_2 T_2, \quad (1.1)$$

$$\rho_1^0, \rho_2^0, R_2, c_{gV}, c_{1p}, c_2 = \text{const},$$

where p , e_1 , e_2 , T_1 , and T_2 are the pressure in the gas, the internal energies, and temperatures of the effective gas and the large particles, ρ_1^0 , ρ_{1p}^0 , and ρ_2^0 are the true densities of the effective gas, the small particles, and the large particles, respectively, R_g is the gas constant, and c_{gV} , c_{1p} , and c_2 are the specific heats of the gas (at constant volume) and the small and large particles. The thermophysical properties of the effective gas R_1 , c_1 and its true density ρ_1^0 can be determined from the relations

$$R_1 = x_{1g} R_g, \quad c_1 = x_{1g} c_{gV} + x_{1p} c_{1p}, \quad x_{1g} + x_{1p} = 1,$$

$$x_{1g} = \rho_{1g} / \rho_1, \quad x_{1p} = \rho_{1p} / \rho_1, \quad \rho_1 = \rho_{1g} + \rho_{1p}, \quad \rho_1 = \alpha_1 \rho_1^0,$$

$$\alpha_1 + \alpha_2 = 1, \quad \alpha_2 = \rho_2 / \rho_2^0, \quad \alpha_1 = \alpha_{1g} + \alpha_{1p}.$$

Here ρ_1 , ρ_{1g} , ρ_{1p} , and ρ_2 are the normalized densities of the effective gas, its two components, and the large particles, and α_1 , α_{1g} , α_{1p} , and α_2 are the corresponding contents of the components of the mixture by volume. We note that if phase transitions do not occur (x_{1p} , $x_{1g} = \text{const}$) and the volume contents of the particles are small ($\alpha_{1p} \ll 1$, $\alpha_2 \ll 1$), the effective gas can be assumed to be calorically ideal [1].

2. ASPECTS OF THE SPECIFIC FORMULATION OF THE PHASE INTERACTION LAWS IN
THE PRESENCE OF SMALL PARTICLES

In determining the force f exerted on a large particle by the effective gas, we assume that it is the sum of two parts: the force of viscous friction with the gas f_μ and the force associated with momentum transfer in collisions with small particles f_c , i.e.,

Chimkent. Tyumen. Translated from *Prikladnaya Mekhanika i Tekhnicheskaya Fizika*, No. 5, pp. 35-40, September-October, 1993. Original article submitted August 18, 1992.

$$f = f_{\mu} + f_c. \quad (2.1)$$

We write the force f_{μ} of interaction of a large particle with the gas in the form [1, 7]

$$f_{\mu} = (\pi d^2/8) \rho_{1g}^0 C_d |v_1 - v_2| (v_1 - v_2), \quad (2.2)$$

$$C_d = 24/Re_{12} + 4.4/Re_{12}^{0.5} + 0.42, \quad Re_{12} = \rho_{1g}^0 d |v_1 - v_2| / \mu_{1g},$$

where d , C_d , and Re_{12} are the diameter, drag coefficient, and Reynolds number of the relative flow around the particle, v_1 and v_2 are the velocities of the gas and the large particles, and μ_{1g} is the dynamic viscosity coefficient of the gas.

By analogy with [1], we determine the interaction force between small and large particles on the assumption that the small particles acquire the velocity of the large particles after collision, i.e., the excess momentum of the small particles $m_p(v_1 - v_2)$ (m_p is the small particle mass) is transferred in collisions. We find the number of particle collisions, starting with the elementary scheme in [1, 6, 8], introducing the correction factor η , which characterizes the fraction of small particles colliding with a large particle (the remaining fraction $1 - \eta$ corresponds to particles that intermingle with the gas flow and move with it toward the head of the large particle, but do not collide with it). We then write the expression for f_c in the form

$$f_c = \eta (\pi d^2/4) \rho_{1p} |v_1 - v_2| (v_1 - v_2), \quad 0 \leq \eta \leq 1. \quad (2.3)$$

The particle collision efficiency η depends on many factors in general (the size and mass contents of small and large particles, their relative velocity, the viscosity of the gas, etc.). Obviously, when the size and concentration of the small particles are small, the coefficient η depends on the dimensionless parameter $St = \ell_V/d$ is the Stokes number (ℓ_V is a characteristic relaxation length of the velocity of a small particle in Stokes flow). A simple empirical relation is given in [9]:

$$\eta(St) = St^2 / (St + 0.125)^2, \quad St \geq 0.1. \quad (2.4)$$

In cases where the motion of the small particles does not obey Stokes' law or their concentration is not small (and the influence of the particles on the gas flow can no longer be ignored), it is difficult to evaluate the factor η (this is a separate and fairly complicated problem).

It should be noted that the influence of the small particles on the force interaction of the phases can sometimes be taken approximately into account by writing the expression for the force of the effective gas on a large particle in a form analogous to (2.2) (with the actual parameters of the gas replaced by the effective parameters of the mixture of the gas with the small particles):

$$f^e = (\pi d^2/8) \rho_1^0 C_d^e |v_1 - v_2| (v_1 - v_2), \quad (2.5)$$

$$C_d^e = 24/Re_{12}^e + 4.4/\sqrt{Re_{12}^e} + 0.42, \quad Re_{12}^e = \rho_1^0 d |v_1 - v_2| / \mu_1$$

(μ_1 is the viscosity coefficient of the effective gas, which can be regarded as equal to the dynamic viscosity coefficient of the gas in the case of not too highly concentrated aerocolloids: $\mu_1 \approx \mu_{1g}$). A comparative analysis of the forces f_{μ} , f_c , and f^e is carried out below.

We represent the incoming heat flux from the carrier phase to a large particle by the expression [1, 7]

$$q = \pi d \lambda_g Nu_{12} (T_1 - T_2), \quad (2.6)$$

$$Nu_{12} = 2 + 0.6 Re_{12}^{0.5} Pr_g^{0.3}, \quad Pr_g = c_{gp} \mu_{1g} / \lambda_g.$$

Here Nu_{12} and Pr_g are the Nusselt and Prandtl numbers, c_{gp} is the specific heat of the gas at constant pressure, and λ_g is its thermal conductivity. Equation (2.6) is written under the assumption that the time of contact between the particles during collisions (when they do not stick together) is sufficiently small in comparison with the characteristic time of heat transfer between them, so that the influence of the small particles on the heat-transfer process between the gas and the large particles can be disregarded.

3. ANALYSIS OF THE FORCE EXERTED BY THE EFFECTIVE GAS ON A LARGE PARTICLE

We carry out a comparative analysis of the forces applied to a large particle by the effective gas. To simplify the estimates, we assume that the collision efficiency is constant: $\eta = \text{const.}$

From Eqs. (2.2) and (2.3) we readily deduce the relation $f_c = (2\eta\rho_{1p}/\rho_{1g}^0 C_d)f_\mu$. We therefore have the following relation for the cases of Stokes ($Re_{12} \ll 1$, $C_d = 24/Re_{12}$) and Newtonian ($Re_{12} \gg 1$, $C_d \approx 0.5$) flow of a not too highly concentrated small-particle aerosol ($\alpha_{1p} \ll 1$, $\alpha_{1g} \approx 1$) around the large particle:

$$\frac{f_c}{f_\mu} \approx \begin{cases} \eta m_{1p} Re_{12}/12, & Re_{12} \ll 1, \\ 4\eta m_{1p}, & Re_{12} \gg 1, \quad m_{1p} = \rho_{1p}/\rho_{1g} \end{cases}$$

(m_{1p} is the relative mass content of small particles in the effective gas). Clearly, in Stokes flow of a gas mixture with not very large mass contents of small particles ($m_{1p} \lesssim 10$) we can assume that $f_c \ll f_\mu$ and disregard the force f_c in the calculations.

The comparison of f_μ and f_c for the case of Newtonian flow is illustrated in Fig. 1. Curve a corresponds to values of m_{1p} and η for which the ratio of the forces f_c and f_μ is $f_c/f_\mu \approx 4\eta m_{1p} \approx 1$. The horizontal lines a' and a'' indicate the boundaries of the domain in the (m_{1p} , η) plane wherein the relation $0.1 \lesssim f_c/f_\mu \lesssim 10$ holds. The sloping lines correspond to the dependence of f_c/f_μ on m_{1p} for different values of η . Clearly, in Newtonian flow around the large particle (as opposed to Stokes flow) the condition $f_c \ll f_\mu$ is satisfied only for values of m_{1p} and η within the narrow zone below the line a''. For $\eta \gtrsim 0.05$ and $m_{1p} \gtrsim 0.5$ the force f_c becomes comparable with or much greater than f_μ in magnitude.

We now compare the different representations of the force exerted by the effective gas on a large particle $f = f_\mu + f_c$ and f^e . From Eqs. (2.1)-(2.3), (2.5) we readily obtain the relation

$$f^e = f C_d \rho_{1g}^0 / (2\eta\rho_{1p} + C_d \rho_{1g}^0). \quad (3.1)$$

Treating separately the cases of Stokes (Re_{12} , $Re_{12}^e \ll 1$) and Newtonian (Re_{12} , $Re_{12}^e \gg 1$) flow of a not too highly concentrated small-particle aerosol around large particles (when it can be assumed that $\alpha_{1p} \ll 1$, $\alpha_{1g} \approx 1$, and $\mu_1 \approx \mu_{1g}$), from Eq. (3.1) we obtain

$$\frac{f^e}{f} \approx \begin{cases} 1 / \left(\frac{\eta}{12} m_{1p} Re_{12} + 1 \right), & Re_{12} \ll 1/(1 + m_{1p}), \\ (1 + m_{1p}) / (1 + 4\eta m_{1p}), & Re_{12} \gg 1. \end{cases}$$

It follows from this result that for sufficiently small Reynolds numbers, when $Re_{12} \ll 1/(m_{1p} + 1)$, it can almost always be assumed that $f^e \approx f$, i.e., the different representations of the force of the effective gas on a large particle according to Eqs. (2.1) and (2.5) yield approximately the same values.

The behavior of the ratio f^e/f as a function of the mass content of small particles m_{1p} for $Re_{12} \gg 1$ is shown in Fig. 2. We see that the values given by Eq. (2.5), which is used to calculate the effective force f^e , are too high for $\eta > 0.25$ and, conversely, are too low for $\eta < 0.25$ in comparison with the results given by Eq. (2.1), where the influence of the small particles on the force exerted by the effective gas on a large particle is taken into account more subtly. It is interesting to note that f and f^e are equal at $\eta = 0.25$: $f = f^e$, regardless of the value of m_{1p} .

We note that a significant difference (twofold or more) between the values of f and f^e is observed in the following intervals of the parameters η and m_{1p} : $\eta \leq (m_{1p} - 1)/8m_{1p}$, $m_{1p} \geq 1$ and $\eta \geq (m_{1p} + 0.5)/2m_{1p}$, $m_{1p} \geq 0.5$.

As an example illustrating the influence of interaction between small and large particles on the flow of a two-fraction (i.e., with two distinct particle sizes) aerosol, we consider the structure of a shock wave.

4. STATEMENT OF THE PROBLEM AND RESULTS OF CALCULATIONS

Let a plane stationary shock wave propagate with a velocity v_{10} in an unbounded space occupied by a mixture of a gas with small and large particles, and let $v_{10} > a_{10}^e$, a_0^e , where a_{10}^e and a_0^e are the preshock equilibrium sound velocities in the mixture of the gas with the small particles and in the complete aerosol with small and large particles ($a_0^e < a_{10}^e < a_{1g0}$, where the latter is the sound velocity in the particle-free gas). The shock wave can be fronted by a discontinuity, at which the parameters of the effective gas satisfy the Rankine-Hugoniot equations, and the parameters of the large particles are practically constant. The parameters of the components of the mixture after the discontinuity determine the boundary

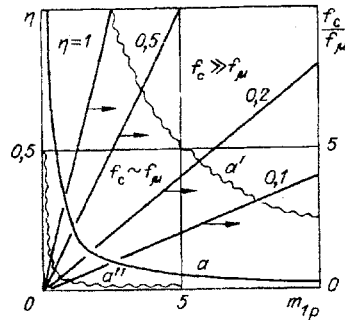


Fig. 1

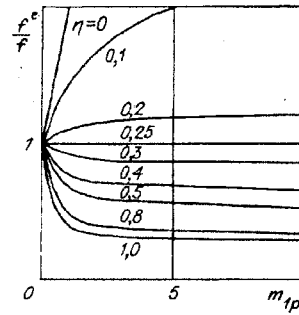


Fig. 2

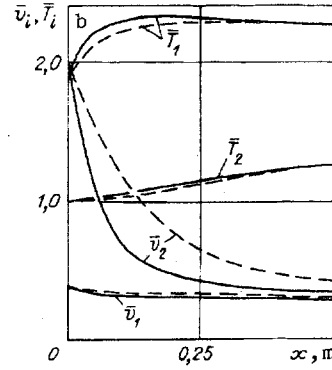
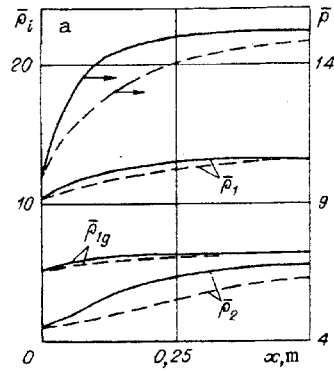


Fig. 3

conditions at a certain point $x = x_f$ corresponding to the position of the frontal discontinuity (compression shock) and can be used to calculate the structure of the relaxation zone in the region $x > x_f$.

When $a_0^e < v_{10} < a_{10}^e$, the shock wave is not fronted by a discontinuity, i.e., the parameters of the mixture in the compression wave vary continuously from the preshock equilibrium state to the postshock equilibrium state. In this case the linear solution of the system of equations of motion of the mixture in the vicinity of the initial preshock state can be used to formulate the boundary conditions. A ranging technique has been used in previous works [3, 4] to calculate the structures of continuous (smeared) shock waves. More comprehensively definition of a problem concerning the structure of the shock wave in suspension of matter in gas is considered in [1, 7].

An analysis of the conditions of similarity of shock wave structures has shown that the following dimensionless parameters are the main criteria of approximate flow similarity in the relaxation zone of the shock wave when collisions occur between small and large particles with a constant efficiency η : the adiabatic exponent of the gas γ_g , the Mach number of the shock wave relative to the sound velocity in the gas $M = v_{10}/a_{1g0}$, the ratio of the specific heats of the small particles and the gas $C_p = c_p/c_{gV}$, the relative preshock mass contents of small and large particles $m_{1p} = \rho_{1p0}/\rho_{1g0}$ and $m_2 = \rho_{20}/\rho_{1g0}$, and the collision efficiency η . When η is variable and depends on St , it is replaced in the set of similarity criteria by the characteristic value of the Stokes number (relative to the sound velocity in the gas) $St_{0S} = \rho_{1p}^0 d_p^2 a_{1g0} / 18 \mu_{1g}$ (d_p is the small particle diameter). If Eq. (2.4) is used to describe the function $\eta(St)$, the efficiency clearly obeys the inequality $\eta \geq 0.8$ and depends weakly on St for $St \geq 1$. Since $St = k Re_{12} / 18$ ($k = \rho_{1p}^0 d_p^2 / \rho_{1g}^0 d^2$), we can assume approximately that $\eta \approx 0.8-1$ in the shock wave, where $Re_{12} \geq 10^3$ for not too small values of k (such that $k Re_{12} \geq 20$). The invariance of the parameter St_{0S} , required for approximate similarity of the shock structures, is no longer essential.

We have investigated the influence of particle interaction and the main governing parameters on the structure of a shock wave in a mixture of air with small and large particles of quartz sand. We assume that the preshock mixture is in thermodynamic equilibrium ($v_{10} = v_{20}$, $T_{10} = T_{20}$) at a pressure of 0.1 MPa. The equations of motion of the aerosol with the closing relations (1.1), (2.1)-(2.6) and appropriate boundary conditions are integrated numerically by a modified Euler method. The computational error is checked against satisfaction of the first integrals of mass, momentum, and energy. The calculations are carried out for waves with relative velocities $M = v_{10}/a_{1g0} = 0.6-2$.

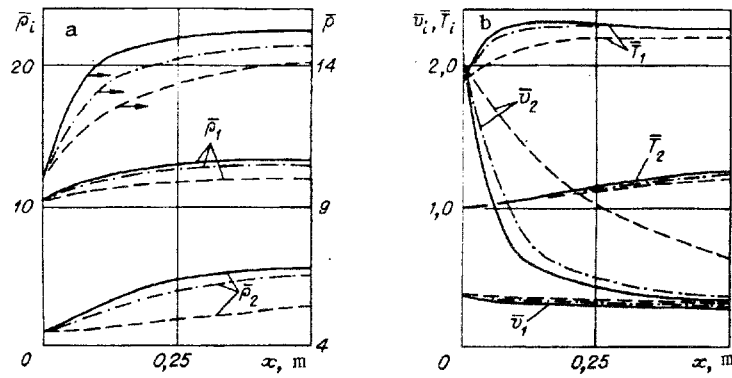


Fig. 4

The relative mass contents of small and large particles m_{1p} and m_2 are varied from 0.5 to 2. The large particle diameter d is varied in the range from 50 μm to 200 μm . The efficiency η is assumed to be constant and is varied from 0 to 1 ($\eta = 0$ corresponds to completely noninteracting particles).

Some results of the calculations are shown in Figs. 3 and 4. The influence of different representations of the interaction force between the effective gas and large particles on the shock structure is illustrated in Fig. 3 (everywhere $\rho_i = \rho_i/\rho_{1g0}$, $v_i = v_i/a_{1g0}$, $p = p/p_0$, and $T_i = T_i/T_{10}$, $i = 1, 2$). The dashed curves indicate the behavior of the parameters of the phases when the particle interaction force is calculated according to Eq. (2.5), and the solid curves represent the same for Eq. (2.1). Here $M = 2$, $m_{1p} = m_2 = 1$, $d = 200 \mu\text{m}$, and $\eta = 0.8$. We see that the use of different equations for f with the indicated values of the governing parameters mainly affects the density and the velocity (Fig. 3a and 3b) of the large particles, where Eq. (2.5) gives high values for the density and low values for the velocity in comparison with Eq. (2.1) over the entire length of the relaxation zone. These disparities are attributable to the fact, obvious from Fig. 2, that for $Re_{12} \gg 1$ (as prevails in a shock wave), $\eta = 0.8$, and $m_{1p} \geq 1$ the approximate ratio of the forces f and f^e calculated according to Eqs. (2.1) and (2.5), respectively, is $f^e/f \leq 0.5$.

Figure 4 illustrates the influence of the efficiency η of collisions between small and large particles on the distribution of the phase parameters in the relaxation zone of a shock wave with a relative velocity $M = 2$ for $m_{1p} = 1$, $m_2 = 1$, and $d = 200 \mu\text{m}$. The dashed, dot-dash, and solid curves correspond to $\eta = 0, 0.5, 0.8$. The increase of η from 0 to 0.8 causes the large particle velocity \bar{v}_2 to decrease considerably, and their density $\bar{\rho}_2$ to increase. This is attributable to the fact that the interaction force between the phases increases with η as a result of the increasing rate of collisions between small and large particles. In this case the large particles after the shock front slow down more rapidly, and their concentration increases. In regard to the parameters of the effective gas, they do not undergo any appreciable variation in the relaxation zone of the shock wave as η increases.

LITERATURE CITED

1. R. I. Nigmatulin, Dynamics of Multiphase Media [in Russian], Part 1, Nauka, Moscow (1987).
2. G. Rudinger, "Some properties of shock relaxation zone in gas flows carrying small particles," Phys. Fluids, 7, No. 5 (1964).
3. R. I. Nigmatulin, "Equations of fluid mechanics and compression shock waves in a two-velocity, two-temperature continuum in the presence of phase transitions," Izv. Akad. Nauk, SSSR, Mekh. Zhidk. Gaza, No. 5 (1967).
4. R. I. Nigmatulin, "Aspects of the hydromechanics of two-phase, polydisperse media," Izv. Akad. Nauk, SSSR, Mekh. Zhidk. Gaza, No. 3 (1968).
5. T. R. Amanbaev and A. I. Ivandaev, "Structure of shock waves in two-phase gas mixtures containing liquid droplets," Prikl. Mekh. Tekh. Fiz., No. 2 (1988).
6. T. R. Amanbaev and A. I. Ivandaev, "Wave propagation in three-phase gas mixtures containing particles and droplets," Prikl. Mekh. Tekh. Fiz., No. 4 (1991).
7. A. I. Ivandaev, A. G. Kutushev, and R. I. Nigmatulin, "Gas dynamics of multiphase media," in: Progress in Science and Technology, Series on Mechanics of Liquids and Gases [in Russian], Vol. 16, VINITI, Moscow (1981).
8. P. C. Reist, Introduction to Aerosol Science, Macmillan, New York (1984).

9. V. N. Uzhov and A. Yu. Val'dberg, Purification of Gases by Wet Filters [in Russian], Khimiya, Moscow (1972).

SPECTRAL COMPOSITION OF WAVE NUMBERS OF LONGITUDINAL VORTICES AND
CHARACTERISTICS OF FLOW STRUCTURE IN A SUPERSONIC JET

V. I. Zapryagaev, S. G. Mironov,
and A. V. Solotchin

UDC 533.6.011

Azimuthal nonuniformities of the distribution of the gasdynamic parameters have been discovered in the supersonic jet issuing from an axisymmetric nozzle in the off-design regime [1-5]. The absence of explanations for the described phenomenon in the works on jets [6-7] indicates the inadequate level of our knowledge of the structure of the supersonic jet. The existence of azimuthal nonuniformities in the initial segment of the jet has been identified, both with the aid of schlieren photographs, on which longitudinal bands are seen, and by direct measurement of the azimuthal distribution of the total pressure in the flow. These nonuniformities show up in jets issuing from nozzles of various dimensions with various gasdynamic parameters, indicating the high frequency of occurrence of this phenomenon, which is observed both in rarefied gas jets [1-2] and in jets at high Reynolds numbers [3-5]. The reproducibility of this phenomenon is confirmed by experiments [8], the results of which basically agree with the conclusions published in [3-5]. The possible cause for the onset of the observed azimuthal nonuniformity may be the coherent vortical formations of the Taylor-Görtler vortex type [3-5] in the shear layer of the jet discharging into a submerged space. This hypothesis is based on comparison of the experimental observations in free jets with the data from the recording of longitudinal vortices in the case of the attachment of both plane [9, 10] and axisymmetric [11, 12] flows. In the case of the discharge of an axisymmetric supersonic jet into a coaxial cylindrical channel with sudden expansion, it is noted that the "primary cause of the formation of longitudinal vortices is loss of stability of the boundary layer upon abrupt rotation of this layer, when the equilibrium between the centrifugal forces and the pressure forces is disrupted" [11]. Longitudinal vortical structures have also been observed in the zone of interaction of the supersonic jet with a liquid [12]. The vortical motion intensifies the mass exchange of the jet with the ambient medium, significantly alters the azimuthal and radial distributions of the total pressure and the Mach number, and also influences the configuration of the jet boundary. The inadequate level of our knowledge of the subject questions leads to the need for further studies of the conditions of the onset and transformation of three-dimensional disturbances in the shear layer of the supersonic jet. An analytic description of the Taylor-Görtler instability in supersonic jets in application to the existing experimental data was presented in [13-16].

In the present work we made a broad experimental study of the observed phenomenon, including probe measurements of the variations of the total pressure, the obtaining of data on the spectral composition of the wave numbers of the spatial nonuniformities, and laser visualization of the jet cross section.

1. The experiments were performed on a jet facility with use of the equipment described in [3-5]. The most significant difference between the present study and that performed previously lies in the use of a rotating nozzle, which made it possible to obtain data on the nature of the azimuthal nonuniformities in the entire jet flow field. In [3-5] the azimuthal angle variation range was 57° , in the present work the range was 360° . Other differences in the measurement technique will be noted below. The phenomenon was studied on an underexpanded supersonic air jet, discharging from an axisymmetric conical nozzle with exit section diameter $d_a = 0.02$ m into a submerged space. The Mach number of the jet at the nozzle exit was $M_a = 1.5$, and the degree of off-design (ratio of the pressure at the nozzle exit to the external pressure) was 4.15. The Reynolds number, based on the characteristic velocity of the jet at the nozzle exit, the dynamic viscosity in the submerged space, and the length of the first cell of the underexpanded jet, was $3.6 \cdot 10^6$.